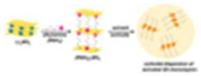

Amine intercalated MS_2 exfoliate in organic solvents to give large 2D nanosheets
4x1mm (600 x 600 DPI)

Journal Name

ARTICLE

Scalable Large Nanosheets of Transition Metal Disulphides through Exfoliation of Amine Intercalated MS_2 [M = Mo, W] in Organic Solvents

Received 00th January 20xx,
Accepted 00th January 20xx

DOI: 10.1039/x0xx00000x

www.rsc.org/

A. Anto Jeffery, C. Nethravathi, Michael Rajamathi*

Various alkylamine intercalated MS_2 (M = Mo, W) have been prepared by reacting Li_xMS_2 with aqueous solutions of the amines. The amine intercalated MS_2 exfoliate readily in alcohols. While the shorter amine intercalated MS_2 exfoliate better in lower alcohols the longer amine intercalated MS_2 exfoliate better in higher alcohols. The longer amine intercalated MS_2 exfoliate well even in a nonpolar solvent, toluene. Up to 9 millimoles of MS_2 per liter could be dispersed through exfoliation in organic solvents. The dispersions are quite stable and comprise 2D–nanosheets of MS_2. Hybrids of MoS_2 and WS_2 could be prepared by evaporating the solvent from a mixture of colloidal dispersions of amine intercalated MoS_2 and WS_2. The hybrid exhibits features of a heterostructure in its photoluminescence spectrum.

Introduction

Two dimensional (2D) materials or nanosheets derived from layered solids are in focus owing to their interesting properties and potential applications in various domains. Subsequent to the discovery of graphene[1,2] and the demonstration of its interesting properties, inorganic nanosheets derived from layered solids such as h-BN,[3] transition metal dichalcogenides[1,3-6] and layered oxides[7,8] have taken prominence. Among these, nanosheets of TMDCs that have strong in-plane bonding and flexibility are of special importance due to their potential applications in electronics, optoelectronics,[4,9] sensing[10] and catalysis.[11-13] While the bulk MS_2 are indirect bandgap semiconductors their 2D analogs have a direct bandgap.[14-16] These nanosheets show excellent photoluminescence,[14] high carrier mobility[17] and high on/off ratios for transistor applications.[18-20] Further, 2D nanosheets are used in the preparation of layered hybrids and heterostructures.[21] TMDC-graphene hybrids exhibit synergetic effects and are used in photoresponsive devices[22] and as battery electrodes.[23,24]

While the small scale preparations of TMDC 2D nanosheets are suitable for electronic devices, large scale production of the same is required for applications such as catalysis and electrochemical energy storage and in the fabrication of heterostructures/hybrids.[25-27] Numerous methods have been developed to produce two dimensional TMDCs. These include mechanical exfoliation using scotch tape,[1] chemical vapour deposition,[28,29] direct chemical synthesis,[30] electrochemical synthesis,[31] liquid phase exfoliation[32-35] and exfoliation in solvents through suitable intercalation[36,37] (chemical exfoliation). Among these methods exfoliation of TMDCs through suitable intercalation would be suitable for the large scale synthesis of monolayer to few layer nanosheets. Depending on the solvent/type, layered materials can be exfoliated after suitable interlayer modification.[36,38,39] Major advantages of chemical exfoliation are the ease of thin film fabrication, nanodevices fabrication and layered hybrid formation through mere stoichiometric mixing of dispersions containing different 2D compounds.[5]

Lithiated MCh_2 (M = Mo, W, T, Ta) and (Ch = S, Se, Te) exfoliate in water due to the highly exothermic reaction between the intercalated Li atoms and water.[40,41] The colloidal dispersions of the 2D TMDC nanosheets thus obtained are quite stable. The problems with this method are that (i) Li_xMCh_2 are highly unstable and have to be stored under inert atmosphere and (ii) lithium compounds remain as impurities in the hybrids prepared starting from the colloidal dispersion. To overcome these difficulties we recently developed a liquid phase exfoliation method through intercalation of NH_3/NH_4^+ in transition metal disulphides, MS_2 (M = Mo, W).[36] In the synthesis of hybrids, it is important to have the two components dispersed in the same solvent. Thus it is important to develop methods to exfoliate TMDCs in diverse solvents. Keeping this in mind we have prepared organic molecule intercalated TMDCs to help exfoliate them in organic solvents. Amines could be intercalated in TMDCs by the procedure similar to the one employed for ammonia intercalation. In this work, we demonstrate the synthesis of a

[a] Materials Research Group, Department of Chemistry, St. Joseph's College, 36 Lalbagh Road, Bangalore 560027, INDIA.

† Footnotes relaoting to the title and/or authors should appear here.
Electronic Supplementary Information (ESI) available: [details of any supplementary information available should be included here]. See DOI: 10.1039/x0xx00000x

series of amine intercalated MS_2 (M = Mo, W) and their excellent exfoliation in organic solvents.

Experimental

Synthesis of Li_xMS_2 (M = Mo, W)

Dry molybdenum disulphide (1g, 6.24 mmol) was stirred with 8 ml of 2.5M solution of *n*-butyllithium in hexane under nitrogen atmosphere at room temperature for 48 h to form lithiated MoS_2.[41] After 48 h, the excess *n*-butyllithium was removed by washing several times with dry *n*-hexane and the product was preserved in dry *n*-hexane under inert atmosphere.

Li_xWS_2 was synthesized by a solvothermal method.[40] 10 ml of 2.5M *n*-butyllithium was added to dry tungsten disulphide (1g, 4.03 mmol) taken in an 80 ml teflon lined autoclave under inert atmosphere and the autoclave was sealed immediately. The autoclave was heated at 90 °C for 24 h in an air oven. After 24 h, the autoclave was opened under nitrogen atmosphere. The lithiated tungsten disulphide was washed several times with dry *n*-hexane to remove the excess *n*-butyllithium and the product was preserved in dry *n*-hexane under inert atmosphere.

Synthesis of amine intercalated MS_2 (M = Mo, W)

Aqueous solutions of a series of small chain to long chain n-alkyl amines like *n*–butylamine (BA), *n*–octylamine (OA), *n*–dodecylamine (DDA), and *n*–octadecylamine (ODA) were prepared by adjusting the pH of the solutions to 7 by adding necessary amounts of dilute HCl. Freshly prepared amine solution was taken in a 100 ml beaker. Under inert atmosphere, about 0.350 g of Li_xMS_2 (M=Mo, W) in *n*-hexane was added to the amine solution and the mixture stirred vigorously for 20 min. The black slurry formed was washed using rectified spirit five times and with water/ethanol (50:50) mixture twice to remove excess amine, filtered and dried at room temperature. The amine-intercalated MS_2 samples are hereafter referred to as BA–MS_2, OA–MS_2, DDA–$MS_2$and ODA–MS_2.

Exfoliation studies

Colloidal dispersion of MS_2 (M = Mo, W) layers in organic solvents were obtained by sonicating 25 mg of amine-MS_2 in 30 ml of the solvent such as ethanol, 1-butanol, 1-hexanol, 1-octanol, and toluene for 2 h. The resultant colloidal dispersion was centrifuged at 1000 rpm for 10 min to remove any undispersed solid. The undispersed solid was washed thrice with acetone, dried in the oven and weighed to constant weight to determine the amount exfoliated in the solvent. The stability of colloidal dispersion was probed by allowing the dispersion to stand undisturbed for several hours to days. At the end of each day, the solid settled was separated from supernatant colloid by centrifugation, washed, dried and weighed. This procedure was repeated until the amount of the settled solid reached greater than or equal to 50% of the weight of the dispersed solid. The time taken for ~50% of the dispersed solid to settle down is taken as the measure of colloidal stability and is represented as the half-life ($t_{1/2}$) of the colloidal dispersion. In some cases, where the stability of the colloidal dispersion was found poor, the settled solids were separated on hourly basis.

Preparation of MoS_2–WS_2 hybrid

The layers from the colloidal dispersions can be recovered by evaporation of the solvent, adding a solvent of different polarity[42] or by high speed centrifugation.[43] We have used the method of evaporation here. About 70 mg each of OA–MoS_2, and OA–WS_2 was dispersed separately in 80ml of 1-octanol. The resultant colloidal dispersions were mixed and the mixture sonicated for 1h. The solvent from the mixture was removed using a rotary evaporator and the residue was dried at 65 °C in an air oven.

About 100 mg of the above hybrid was heated at 500 °C for 4 h under inert atmosphere to deaminate it. The product was washed with water, followed by ethanol and dried at 65 °C in an air oven.

Characterization

Samples were analyzed by recording PXRD patterns using PANalytical X'pertpro diffractometer (Cu Kα radiation, secondary graphite monochromator, scanning rate of 1° 2θ/min). Transmission electron microscopy (TEM) images were recorded using a JEOL F3000 microscope operated at 300 kV. The nanoplatelets of MS_2 obtained through exfoliation were characterized by atomic force microscopy (AFM) using APER A100 atomic force microscope in tapping mode. Sample for AFM analysis was prepared by spin coating an aqueous colloidal dispersion of MS_2 onto a Si substrate. X-ray photoelectron spectroscopy (XPS) measurements were carried out with an ESCALab220i-XL spectrometer using a twin-anode Al Kα (1486.6 eV) X-ray source. All spectra were calibrated to the binding energy of the C1s peak at 284.51 eV. The base pressure was around 3×10^{-7} Pa. Photoluminescence (PL) spectra were recorded using a LS 55 Fluorescence spectrometer (Perkin Elmer) at excitation wavelength of 350 and 400 nm.

Results and Discussion

Alkylamines were intercalated in MS_2 by the process described in Figure 1. When lithiated MS_2 were reacted with alkylamine solutions a vigorous reaction ensued leading to the formation of amine-intercalated MS_2. The increased basal spacings observed for the amine intercalated MS_2 compared to pristine MS_2 confirm intercalation of amines in the interlayer of MS_2 (Figure 2). The increase in basal spacing depends on the chain length of the amine and its interlayer orientation. Similar basal spacings are observed for a given amine in both MoS_2 and WS_2. While the basal spacing for the BA–MS_2 is ~10 Å (an increase of ~4 Å from the basal spacing of the pristine MS_2), it is ~33 Å for the ODA–MS_2 (an increase of ~27 Å from the basal spacing of the pristine MS_2). The non-linear increase in basal spacing with chain length of the amine is due to the fact that the orientations of the intercalated amines in the interlayer are different. While the alkyl chains of long chain amines orient themselves perpendicular to the layers, those of the shorter amines have a tilted orientation. Amine intercalation results in

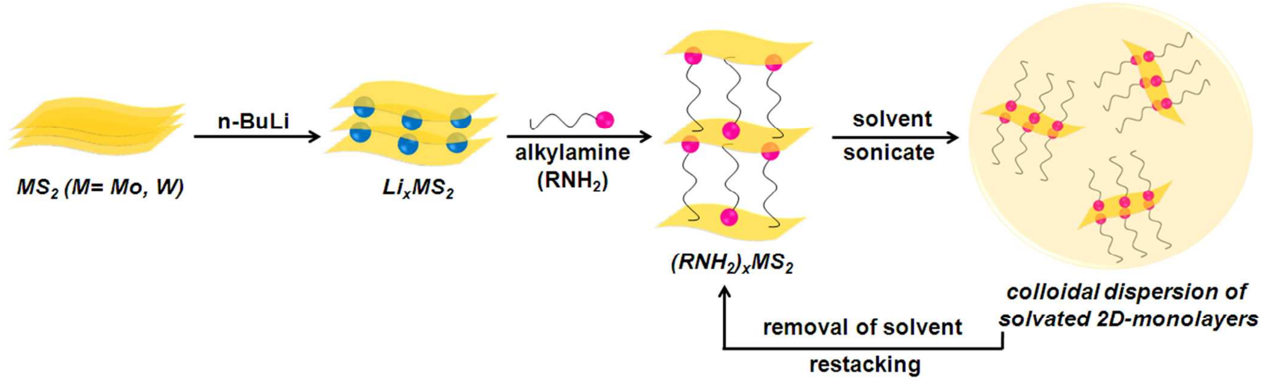

Figure 1 Schematic representation of amine intercalation and exfoliation

turbostratic disorder as indicated by the broad asymmetric peaks starting at 2θ = 32° and 57° in the PXRD patterns of all the intercalated products.

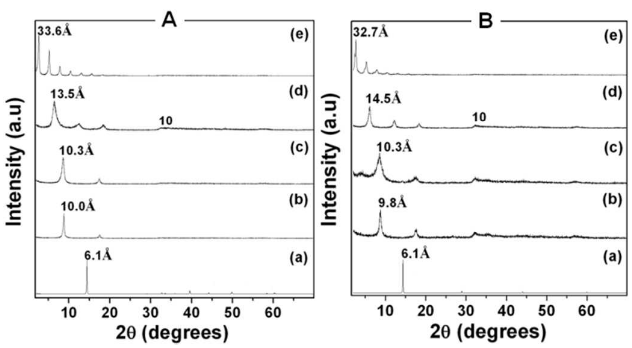

Figure 2 (A) PXRD patterns of the amine intercalated molybdenum disulphide (a) pristine MoS_2, (b) BA–MoS_2, (c)OA–MoS_2, (d) DDA–MoS_2, (e) ODA–MoS_2; (B) PXRD patterns of the amine intercalated tungsten disulphide, (a) pristine WS_2, (b) BA–WS_2, (c) OA–WS_2, (d) DDA–WS_2, (e) ODA–WS_2.

Table 1 Compositions of amine intercalated MS_2 (M=Mo, W) derived from CHNS analysis.

Sample	Mass percentage			Approximate Formula
	Carbon	Nitrogen	Sulphur	
BA–MoS_2	6.54	1.95	33.17	MoS_2·0.27(C_4H_9N)
OA–MoS_2	11.65	1.61	31.40	MoS_2·0.24($C_8H_{19}N$)
ODA–MoS_2	34.29	2.03	21.46	MoS_2·0.45($C_{18}H_{39}N$)
BA–WS_2	4.82	1.57	20.39	WS_2·0.33(C_4H_9N)
OA–WS_2	8.82	1.36	20.61	WS_2·0.29($C_8H_{19}N$)
ODA–WS_2	34.61	2.12	13.69	WS_2·0.73($C_{18}H_{39}N$)

The results of CHNS analysis of the amine-intercalated MS_2 are shown in Table 1. The approximate chemical formulas were computed by comparing the percentages of carbon and nitrogen with that of sulphur. This approximate calculation suggests that 0.24 to 0.43 moles of the amine get intercalated per mole of MoS_2. The extent of intercalation seems to increase with the increase in the chain length of the amine. The extent of amine intercalation is better in the case of WS_2 as we observe higher number of moles of intercalated amine compared to MoS_2 for any given amine.

In order to understand the state of the intercalated amine – whether it is free amine or protonated – and the extent of defects we carried out XPS analysis of the samples and the results are presented in Figure 3 and 4. In the case of lower amine intercalated MoS_2 (BA–MoS_2) the extent of defects is quite high. In the Mo core level spectrum (Figure 3) we observe Mo^{6+} related peaks in addition to those due to Mo^{4+}. In the S core level spectrum, in addition to the peaks due to S^{2-} we observe a peak due to sulphur bonded to oxygen. The intercalated amine exists both as free amine and as alkyl ammonium ion. As we increase the chain length of the amine there are discernible changes in the spectra. The defects decrease with increase in the chain length of the intercalated amine. In the Mo core level spectrum the peaks due Mo^{6+} become weaker in the case of OA–MoS_2 and these are totally absent in the case of DDA–MoS_2. Correspondingly in the S core level spectrum the intensity of the peak due to sulphur bonded to oxygen go on decreasing as the chain length is increased and the peak is absent in the case of DDA–MoS_2. However, the nature of the intercalated species is the same in all the cases – the intercalated amine exists both as free amine and alkyl ammonium ion, whatever is the intercalated amine.

As W is more prone to oxidation compared to Mo, we observe more intense peaks due to W^{6+} in the W core level spectrum of BA–WS_2 and correspondingly a stronger peak due to sulphur bonded to oxygen in the S core level spectrum (Figure 4). Though, as in the case of MoS_2, the extent of defects decreases with increase in the chain length of the intercalated amine, the defects do not vanish completely as indicated by weak peaks due to W^{6+} in the W core level spectrum of DDA–WS_2.

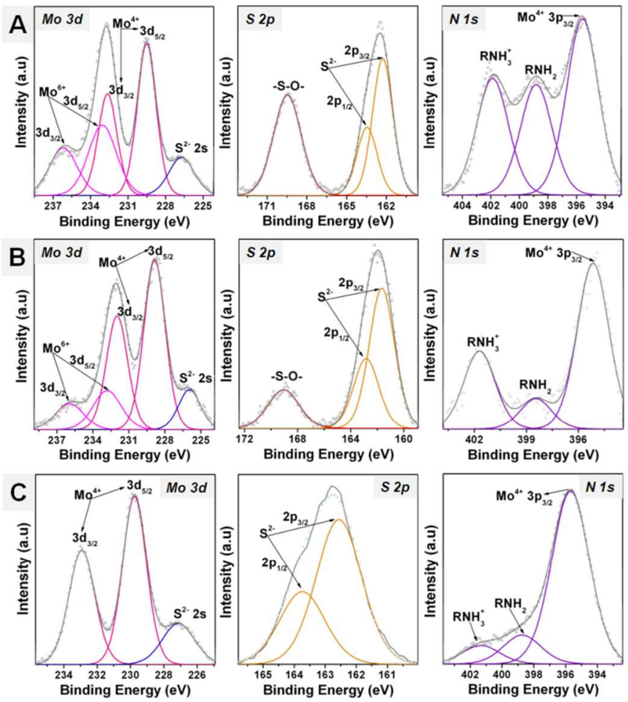

Figure 3 Mo, S and N core level X-ray photoelectrons spectra of (A) BA–MoS_2, (B) OA–MoS_2, (C) DDA–MoS_2.

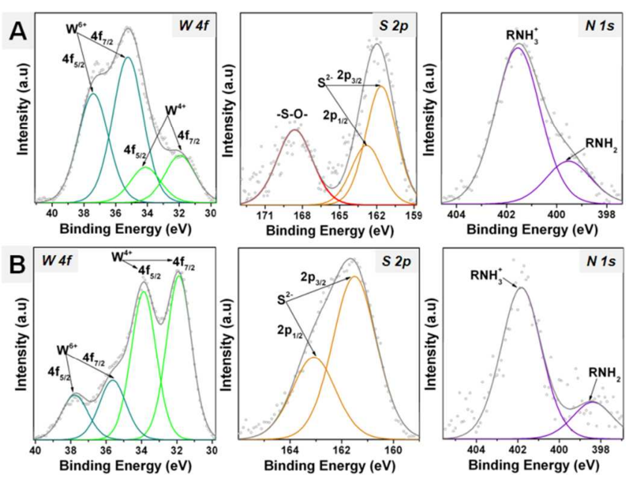

Figure 4 W, S and N core level X-ray photoelectrons spectra of (A) BA–WS_2, (B) DDA–WS_2.

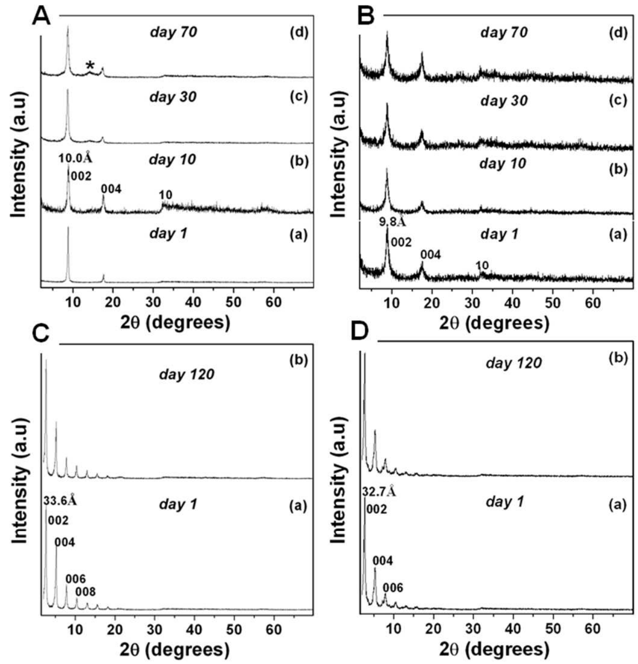

Figure 5 PXRD patterns [A] of BA–MoS_2, [B] BA–WS_2, [C] ODA–MoS_2 and [D] ODA–WS_2 kept standing for various durations at room temperature.

The control over defects by the chain length of the alkylamine is interesting and it could be used to engineer the extent of defects in amine-MS_2 and hence on the nanosheets derived from them. The decrease in defects with increase in the chain length of amines can be attributed to lower reactivity of longer amines leading to less exothermic conditions.

One of the problems with ammoniated MS_2 is their poor shelf-life.[36] These were unstable when stored at room temperature and lost the intercalated ammonia within days. In order to see if instability is an issue for the amine intercalated MS_2 too, we studied the room temperature stability of BA–MS_2 and ODA–MS_2 (M=Mo,W) by allowing the samples to stand several days to months. The PXRD analysis was carried out on daily basis to probe any changes. Figure 5 shows the PXRD patterns of the BA–MS_2 and ODA–MS_2 (M = Mo, W) systems stored in non-air-tight containers for different durations. From the evolution of the PXRD patterns of BA–MoS_2 with time (Figure 5A) it is clear that the compound is stable up to 70 days. Beyond 70 days, the PXRD pattern of n-BA/MoS_2 shows a weak peak due to the *002* reflection of pristine MoS_2 (marked in asterisk in Figure 5A). This stability is far superior to what was observed in the case of ammoniated MoS_2.[36] The PXRD pattern of BA–WS_2 remains the same even after 70 days (Figure 5B) indicating that it is very stable under ambient conditions. Stability increases with the chain length of the intercalated amine. The PXRD patterns of ODA–MS_2 (M=Mo, W) after 120 days is identical to those of the as prepared samples (Figure 5C and D).

ARTICLE

Table 2 Extent of exfoliation and the stability of the colloidal dispersions of amine intercalated MS_2

Amine–MS_2	ethanol		1-butanol		1-hexanol		1-octanol		toluene	
	A[a]	T[b]	A	T	A	T	A	T	A	T
BA–MoS_2	3.2	72	2.4	60	2.6	58	2.7	3	-	-
OA–MoS_2	2.8	24	3.6	24	3.7	24	5.1	8	1.7	8
DDA–MoS_2	2.6	24	3.5	32	5.0	32	8.0	36	2.5	20
ODA–MoS_2	2.8	4	4.0	24	7.0	32	9.0	76	3.8	48
BA–WS_2	4.1	96	3.5	80	2.5	146	2.9	146	-	-
OA–WS_2	2.4	96	2.5	48	2.5	48	3.6	24	0.2	8
DDA–WS_2	1.8	48	2.6	48	3.0	288	3.2	408	0.3	8
ODA–WS_2	3.0	4	4.0	48	5.0	72	7.0	96	3.2	12

[a]A = Amount exfoliated ($mmol/dm^3$); [b] T = $t_{1/2}$ (h)

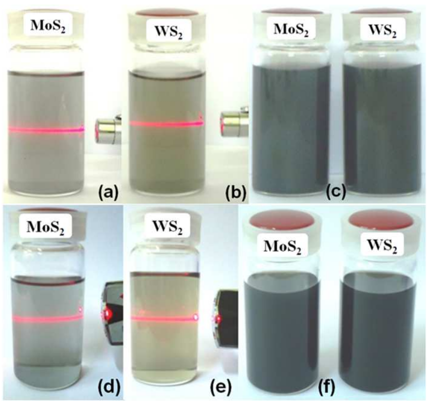

Figure 6 Photographs of the colloidal dispersions of BA–MS_2 (a, b and c) and ODA–MS_2 (d, e and f) in 1-butanol. The dispersions exhibit Tyndall effect (a, b, d and e).

All the amine intercalated MS_2 exfoliate well in alcohols and the colloidal dispersions of exfoliated layers are quite stable and exhibit Tyndall effect (Figure 6). We list the number of millimoles of the amine intercalated MS_2 that get dispersed per litre of the solvent and the time taken for 50% of the dispersed material to flocculate ($t_{1/2}$) in Table 2. From this data we can arrive at the following conclusions. (1) The shorter amine intercalated MS_2 exfoliate better in lower alcohols and the longer amine intercalated MS_2 exfoliate better in higher alcohols. (2) The stability of the colloidal dispersions of exfoliated WS_2 is higher than that of MoS_2. (3) Longer amine intercalated MS_2 exfoliates in toluene, a non-polar solvent, with the extent of exfoliation and the stability of dispersion increasing with increase in the chain length of the intercalated amine.

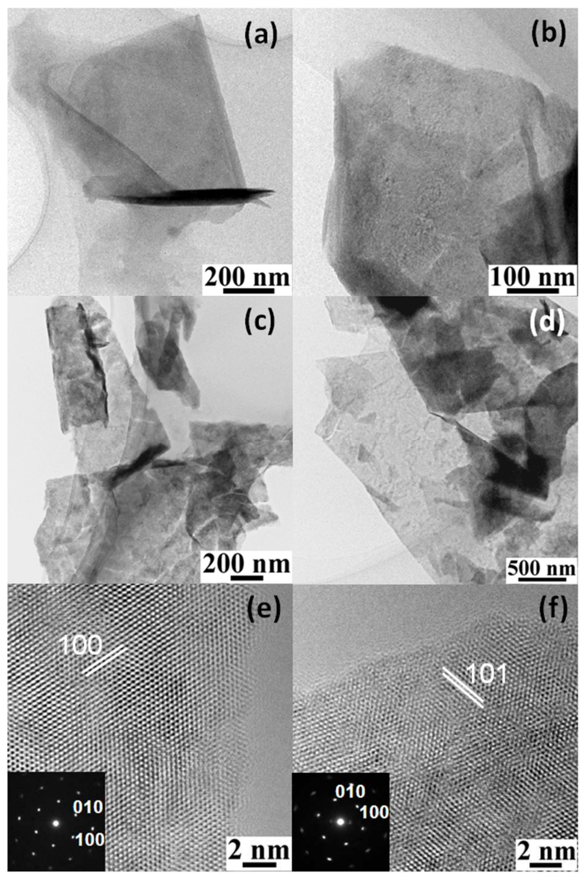

Figure 7 Bright field TEM images of exfoliated layers of BA–MoS_2 (a, b) and BA–WS_2 (c, d) and the HRTEM images of a layer each of BA–MoS_2 (e) and BA–WS_2 (f).

Exfoliation of amine intercalated MS_2 in alcohols operates through solvation of layers and the alkyl chains of the intercalated amines. The alkyl groups of amine surfactant interact with the nonpolar alkyl chains of the alcohols and the inorganic layer is solvated by the polar hydroxyl groups of alcohol. Increasing the chain length of the intercalated amine increases the interaction with the alkyl chains of the alcohols leading to efficient exfoliation.

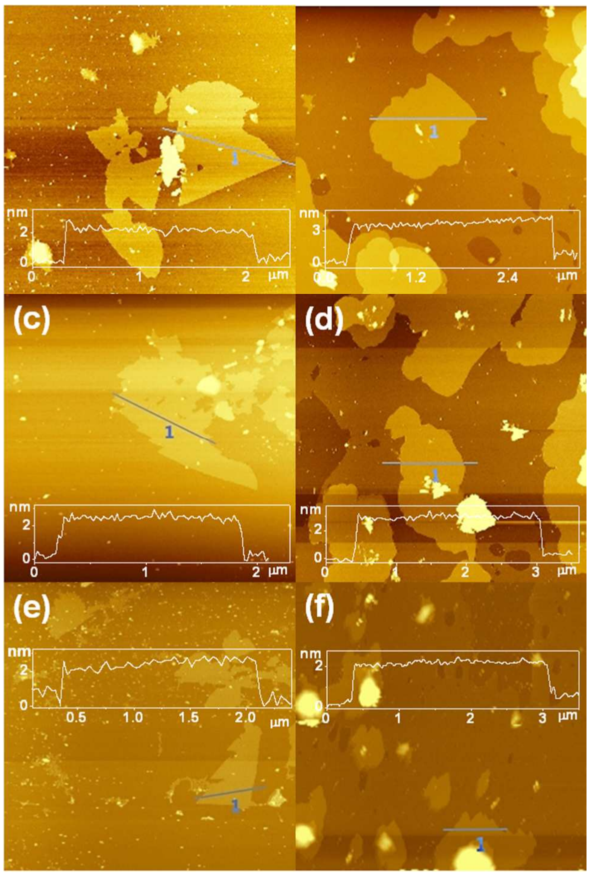

Figure 8 AFM images and thickness profiles of the 2D nanosheets of amine intercalated MS_2 deposited on Si/SiO_2 substrate by evaporating a drop of the colloidal dispersion of the exfoliated layers in 1-butanol. (a) BA–MoS_2, (b) BA–WS_2, (c) OA–MoS_2 (d) OA–WS_2, (e) ODA–MoS_2, and (f) ODA–WS_2.

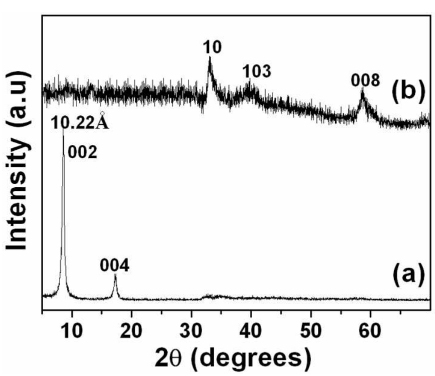

Figure 9 PXRD patterns of OA–MoS_2/WS_2 hybrid before (a) and after (b) deamination.

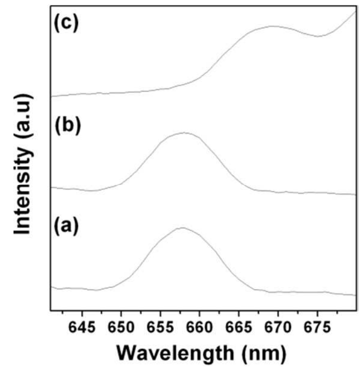

Figure 10 Photoluminescence spectra of (a) MoS_2 nanosheets (b) WS_2 nanosheets, (c) deaminated MoS_2/WS_2 hybrid.

The colloidal dispersions of the exfoliated amine intercalated MS_2 comprise monolayers of the layered solid. The TEM images of the sample deposited on the grid from the colloidal dispersions of octylamine intercalated MS_2 (Figure 6 a-d) show thin sheets that are folded around their edges. The high resolution images of these sheets (Figure 6 e, f) reveal the crystalline nature of these sheets. Lattice fringes due to the (*100*) and (*101*) lattice planes are observed in the case of octylamine intercalated MoS_2 and WS_2 respectively (Figure 6 e, f). The electron diffraction patterns obtained from these layers (insets in Figure 7e and f) could be indexed to hexagonal MoS_2 and WS_2 respectively with the observed spots corresponding to the d spacings of *010* and *100* reflections. The AFM images of the samples deposited on a Si substrate from the colloidal dispersions (Figure 7) further confirm excellent exfoliation. The nanosheets are quite large in the lateral dimensions while the thickness of these sheets is 2 – 3 nm.

The nanosheets of MoS_2 and WS_2 could be costacked by evaporating the solvent from a mixture of the dispersions of amine intercalated MoS_2 and WS_2 to form MoS_2/WS_2 hybrids. The PXRD pattern of MoS_2/WS_2 hybrid obtained from OA–MS_2 (Figure 9a) shows a basal spacing of 10.2 Å, which is the same as the basal spacing of OA–MS_2 (Figure 2A, c and 2B, c). When the hybrid was deaminated by heating at 500 °C, the *00ℓ* reflections are absent in the PXRD pattern with only the in-plane *hk0* reflections observed (Figure 8b) indicating an exfoliated state.

The photoluminescence (PL) spectrum of the deaminated MoS_2/WS_2 hybrid (Figure 10) shows that the A exitonic emission peak of the hybrid is red-shifted and the emission intensity increased compared to the MoS_2 or WS_2 nanosheets. These features are as expected from heterostructures of MoS_2 and WS_2.[36,44,45]

Conclusions

Amine intercalated MS_2 could be prepared by a procedure adapted from our earlier work on the preparation of ammoniated MS_2.[36] The advantages of amine intercalation are three-fold. Firstly it allows exfoliation and nanosheet dispersion in organic solvents. Secondly, the amine-MS_2 have a much longer shelf-life compared to ammoniated MS_2. More importantly, it also allows a control over the extent of chemical defects in the nanosheets. The nanosheets could be assembled to form MoS_2/WS_2 hybrids with heterostructure features.

Acknowledgements

This work was funded by DST, India.

Notes and references

1 K. Novoselov, D. Jiang, F. Schedin, T. Booth, V. Khotkevich, S. Morozov and A. K. Geim, *Proc. Nat. Acad. Sci. U.S.A.,* 2005**,** **102**, 10451-10453.
2 K. S. Novoselov, A. K. Geim, S. V. Morozov, D. Jiang, Y. Zhang, S. V. Dubonos, I. V.; Grigorieva and A. A. Firsov, *Science,* 2004, **306**, 666-669.
3 M. S. Xu, T. Liang, M. M. Shi and H. Z. Chen, *Chem. Rev.*, 2013, **113**, 3766-3798.
4 Q. H. Wang, K. K. Zadeh, A. Kis, J. N. Coleman and M. S. Strano, *Nat. Nanotechnol.,* 2012, **7**, 699-712.
5 M. Chhowalla, S. H. Shin, G. Eda, J. L. Li, P. K. Loh and H. Zhang, *Nat. Chem.,* 2013, **5**, 263-275.
6 I. Song, C. Park and H. C. Choi, *RSC Adv.*, 2015, **5**, 7495-7514.
7 T. Sasaki and M. Watanabe, *J. Am. Chem. Soc.,* 1998, **120**, 4682-4689.
8 M. Osada and T. Sasaki, *Adv. Mater*., 2012, **24**, 210-228.
9 W. Liu, X. Yang, Y. Zhang, M. Xu and H. Chen, *RSC Adv.*, 2014, **4**, 32744-32748.
10 F. K. Perkins, A. L. Friedman, E. Cobas, P. M. Campbell, G. G. Jernigen and B. T. Jonker, *Nano Lett.,* 2013, **13**, 668–673.
11 J. Deng, W. Yuan, P. Ren, Y. Wang, D. Deng, Z. Zhang and X. Bao, *RSC Adv.*, 2014, **4**, 34733-34738.
12 X. Sun, J. Dai, Y. Guo, C. Wu, F. Hu, J. Zhao, X. Zeng and Y. Xie *Nanoscale,* 2014, **6**, 8359-8367.
13 J. Li, X. Liu, L. Pan, W. Qin, T. Chen and Z. Sun, *RSC Adv.*, 2014, **4**, 9647-9651
14 G. Eda, H. Yamaguchi, D. Voiry, T. Fujita, M. Chen and M. Chhowalla, *Nano Lett*., 2011, **11**, 5111-5116.
15 Q. Ji, Y. Zhang, T. Gao, Y. Zhang, D. Ma, M. Liu, Y. Chen, X. Qiao, P. H. Tan, M. Kan, J. Feng, Q. Sun and Z. Liu, *Nano Lett.,* 2013, **13**, 3870–3877.
16 A. Splendiani, L. Sun, Y. Zhang, T. Li, J. Kim, C. Y. Chim, G. Galli and F. Wang, *Nano Lett.,* 2010, **10**, 1271–1275.
17 M. M. Perara, M. W. Lin, H. J. Chuang, B. P. Chamlagain, C. Wang, X. Tan, M. M. C. Cheng, D. Tomanek and Z. Zhou, *ACS Nano,* 2013, **7**, 4449-4458.
18 T. Roy, M. Tosun, J. S. Kang, A. B. Sacid, S. B. Desai, M. Hettick, C. C. Hu and A. Javey, *ACS Nano,* 2014, **8**, 6259-6264.
19 Z. Yin, H. Li, H. Li, L. Jiang, Y. Shi, Y. Sun, G. Lu, Q. Zhang, X. Chen and H. Zhang, *ACS Nano,* 2012, **6**, 74-80.
20 M. Tosun, S. Chuang, H. Fang, A. B. Sacid, M. Hettick, Y. Lin, Y. Zeng and A. Javey, A. *ACS Nano,* 2014, **8**, 4948-4953.
21 A. K. Geim and I. V. Grigorieva, *Nature,* 2013, **499**, 419-425.
22 L. Yu, Y. H. Lee, X. Ling, E. J. G. Santos, Y. C. Shin, Y. Lin, M. Dubey, E. Kaxiras, J. Kong, H. Wang and T. Palacious, *Nano Lett.,* 2014, **14**, 3055–3063.
23 L. Zhang, W. Fan, W. Tjiu and T. Liu, *RSC Adv.*, 2015, **5**, 34777-34787
24 Z. Wang, T. Chen, W. Chen, K. Chang, L. Ma, G. Huang, D. Chen and J. Y. Lee, *J. Mater. Chem. A*, 2013, **1**, 2202-2210.
25 F. Withers, H. Yang, L. Britnell, A. P. Rooney, E. Lewis, A. Felten, C. R. Woods, V. S. Romaguera, T. Georgiou, A. Eckmann, Y. J. Kim, S. G. Yeates, S. J. Haigh, A. K. Geim, K. S. Novoselov and C. Casiraghi, *Nano Lett.,* 2014, **14**, 3987-3992.
26 S. Min and G. Lu, *J. Phys. Chem. C,* 2012, **116**, 25415–25424.
27 A. V. Powell, L. Kosidowski and A. Mcdowall, *J. Mater. Chem.,* 2001, **11**, 1086-1091.
28 Y. H. Lee, X. Q. Zhang, W. Zhang, M. T. Chang, C. T. Lin, K. D. Chang, Y. C. Yu, J. T. W. Wang, C. S. Chang, L. J. Li and T. W. Lin, *Adv. Mater.,* 2012, **24**, 2320-2325.
29 J. K. Huang, J. Pu, C. L. Hsu, M. H. Chiu, Z. Y. Juang, Y. H. Chang, W. H. Chang, Y. Iwasa, T. Takenobu and L. J. Li, *ACS Nano,* 2014, **8**, 923–930.
30 S. Jeong, D. Yoo, J. T. Jang, M. Kim and J. Cheon, *J. Am. Chem. Soc.,* 2012, **134**, 18233–18236.
31 Q. Li, J. T. Newberg, J. C. Walter, J. C. Hemminger and R. M. Penner, *Nano Lett*., 2004, **4**, 277-281.
32 J. N. Coleman, M. Lotya, A. O'Neill, S. D. Bergin, P. J. King, U. Khan, K. Young, A. Gaucher, S. De, R. J. Smith, et al. *Science,* 2011, **331**, 568-571.
33 R. Bari, D. Parviz, F. Khabaz, C. D. Klaassen, S. D. Metzler, M. J. Hansen, R. Khare and M. J. Green. *Phys. Chem. Chem. Phys.,* 2015, **17**, 9383-9393.
34 L. Dong, S. Lin, L. Yang, J. Zhang, C. Yang, D. Yang and H. Lu. *Chem. Commun.,* 2014, **50**, 15936-15939.
35 D. V. Thanh, C.-C. Pan, C.-W. Chuand and K.-H. Wei, *RSC Adv.,* 2014, **4**, 15586-15589.
36 A. A. Jeffery, C. Nethravathi and M. Rajamathi, *J. Phys. Chem. C*, 2014, **118**, 1386-1396.
37 A. U. Liyanage and M. M. Lerner, *RSC Adv.*, 2014, **4**, 47121-47128
38 Z. Tang, Q. Wei and B. A. Guo, *Chem. Commun.,* 2014, **50**, 3934-3937.
39 C. Nethravathi, A. A. Jeffery, M. Rajamathi, N. Kawamoto, R. Tenne, D. Golberg and Y. Bando, *ACS Nano*, 2013, **7**, 7311–7317
40 D. Yang and R. F. Frindt, *J. Phys. Chem. Solids,* 1996, **57**, 1113-1116.
41 M. B. Dines, *Mat. Res. Bull*., 1975, **10**, 287-292.
42 C. Nethravathi, G. Harichandran, C. Shivakumara, N. Ravishankar, M. Rajamathi, *J. Colloid Interface Sci.,* 2005, **288,** 629-633.
43 L. Hu, R. Ma, T. C. Ozawa, T. Sasaki, *Chem. Asian. J.*, 2010, **5**, 248-251.
44 X. Hong, J. Kim, S. F. Shi, Y. Zhang, C. Jin, Y. Sun, S. Tongay, J. Wu, Y. Zhang and F. Wang, *Nat. Nanotech*., 2014, **9**, 682-686.
45 K. Kośmider and J. F.–Rossier, *Phys. Rev. B,* 2013, 87, 075451–075454.